Journal of Sound and Vibration (2002) **256**(3), 533–549
doi:10.1006/jsvi.5009, available online at http://www.idealibrary.com on IDEAL®

FREE VIBRATION ANALYSIS OF ARBITRARILY SHAPED PLATES WITH A MIXED BOUNDARY CONDITION USING NON-DIMENSIONAL DYNAMIC INFLUENCE FUNCTIONS

S. W. KANG

Department of Mechanical Systems Engineering, Hansung University, 389, 2-*ga*, *Samsun-dong*, *Sungbuk-gu Seoul*, 136-792, *Korea*. *E-mail*: *swkang@hansung.ac.kr*

(*Received* 2 *July* 2001, *and in final form* 18 *February* 2002)

A new approach using the non-dimensional dynamic influence functions has been developed for free vibration analysis of arbitrarily shaped plates with a mixed boundary condition involving both simply supported edges and clamped ones. Since the proposed method is based on the collocation method using one-dimensional and wave-type functions, no integration procedure is needed on boundary edges of the plate of interest and numerical calculation schemes are relatively concise. In order to settle the incompleteness of the system matrix, which is due to the discarding of a complex natural boundary condition at simply supported edges, an additional simple equation is devised by means of using a geometric approximation on curved edges. Finally, verification examples show that a complete system matrix formed in this way successfully gives accurate eigenvalues compared with FEM (ANSYS) and other methods.

1. INTRODUCTION

The so-called boundary point method using the non-dimensional dynamic influence functions was developed by the author for arbitrarily shaped membranes [1, 2], two-dimensional acoustic cavities [3], concave membranes [4] and plates with the clamped boundary condition [5]. Research related to the above topics shows that the method is simpler and more accurate than other numerical methods such as the finite element method and the boundary element method. In this paper, the boundary point method that has so far been developed by the author is extended to free vibration analysis of arbitrarily shaped plates with a mixed boundary condition, involving simply supported edges and clamped edges.

A great deal of research for fixed membranes or simply supported plates has been performed in that the associated theoretical formulations are relatively simple compared to plates with other boundary conditions [6–14]. For plates with clamped edges, Durvasula [15] studied a new method for the natural frequencies and mode shapes of clamped skew plates and Hasegwa [16] calculated the fundamental natural frequency of a clamped skew plate using polynomials and the Rayleigh–Ritz method. Also, Hamada [17] obtained a lower bound for the fundamental frequency of a rhombic plate. In the case of the mixed boundary condition involving simply supported edges and clamped edges, Nair [18] dealt with the vibration problems of skew plates with different edge conditions involving simple support and clamping by using the variational method of Ritz. Leissa [19] summarized the numerical results for natural frequencies of rectangular plates for all 21 possible

0022-460X/02/$35.00

combinations of the three elementary boundary conditions (simply supported, clamped, and free boundary conditions). Also, Dickinson [20] extracted an approximate closed-form solution for rectangular plates with various elementary boundary conditions. Furthermore, research on the use of conformal mapping and variational methods for vibrations and bucking of membrane and plates has been carried out [21–24].

Although many application methods have been developed for plates with various types of mixed boundary conditions, they dealt with plates with special shapes such as a rectangle, a parallelogram, and a regular polygon. In this paper, a general method is proposed to obtain the eigenvalues of arbitrarily shaped plates with various combinations of mixed boundary conditions involving simply supported edges and clamped edges. In the procedure of theoretical development, only three boundary conditions of four boundary conditions needed for the mixed boundary condition are used to obtain a system matrix for eigenvalues. A natural boundary condition for simply supported edges is discarded to avoid the difficulties of measuring the curvatures of edges and calculating higher differential terms. On the other hand, an additional simple condition is intuitively devised for completing an incomplete system matrix, which is formed using the three boundary conditions.

Eigenvalues of arbitrarily shaped plates with the mixed boundary condition are obtained from a complete system matrix made by merging the devised additional condition into the incomplete system matrix. Although the complete system matrix gives spurious eigenvalues as well as correct eigenvalues, the spurious ones are discriminated in a special way, which was proposed by the author [5]. Furthermore, verification examples show that the eigenvalues calculated by the proposed method are in good agreement with those given by FEM (ANSYS), Nair's method [18], and Leissa's method [19].

2. GOVERNING EQUATION AND BOUNDARY CONDITIONS

The governing differential equation for free flexural vibrations of an isotropic homogeneous thin plate can be written as

$$D\nabla^4 w + \rho_s \frac{\partial^2 w}{\partial t^2} = 0, \tag{1}$$

where $w = w(\mathbf{r}, t)$ is the transverse deflection at position vector $\mathbf{r}$, ρ_s is the plate density per unit area, and $D = Eh^3/12(1 - \nu^2)$ is the flexural rigidity.

Assuming harmonic motion $w(\mathbf{r}, t) = W(\mathbf{r})e^{j\omega t}$ where ω denotes the circular frequency, equation (1) yields

$$\nabla^4 W - \Lambda^4 W = 0, \quad \Lambda = \left(\frac{\rho_s \omega^2}{D}\right)^{1/4}. \tag{2, 3}$$

In Figure 1, the domain Ω of a plate is bounded by the boundary Γ, which is subject to a mixed boundary condition for simply supported edges Γ_s (dotted contour) and clamped edges Γ_c (solid contour). Then, boundary conditions on Γ can be written as [25]

$$W(\mathbf{r}) = 0 \qquad \frac{\partial^2 W(\mathbf{r})}{\partial n^2} + \frac{\nu}{R}\frac{\partial W}{\partial n} = 0 \quad \text{on } \Gamma_s, \tag{4, 5}$$

$$W(\mathbf{r}) = 0, \qquad \frac{\partial W(\mathbf{r})}{\partial n} = 0 \quad \text{on } \Gamma_c, \tag{6, 7}$$

where equation (5) is a natural boundary condition and equations (4, 6, 7) are geometric boundary conditions.

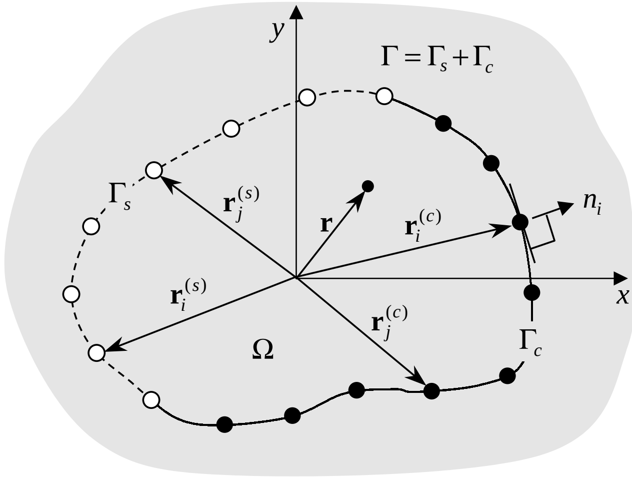

Figure 1. An arbitrarily shaped plate whose boundary consists of the simply supported boundary Γ_s (dotted contour) and the clamped boundary Γ_c (solid contour): each boundary is discretized with boundary points (source points are located at the same positions as the boundary points).

3. THEORETICAL FORMULATION

In a previous research on free vibration analysis of clamped plates [5], a general solution of a clamped plate of the same shape as both contours depicted in Figure 1 was assumed as a linear superposition of the non-dimensional dynamic influence functions (NDIFs) defined in an infinite plate, i.e.,

$$W(\mathbf{r}) = \sum_{j=1}^{N} \{A_j J_0(\Lambda|\mathbf{r} - \mathbf{r}_j|) + B_j I_0(\Lambda|\mathbf{r} - \mathbf{r}_j|)\}, \tag{8}$$

where N denotes the number of source points distributed along the boundary of a clamped plate on an infinite domain. In this paper, equation (8) is also employed as a general solution of a plates with the mixed boundary condition and is divided into two parts according to locations of source points, i.e.,

$$W(\mathbf{r}) = \sum_{j=1}^{Ns} \{A_j^{(s)} J_0(\Lambda|\mathbf{r} - \mathbf{r}_j^{(s)}|) + B_j^{(s)} I_0(\Lambda|\mathbf{r} - \mathbf{r}_j^{(s)}|)\}$$
$$+ \sum_{j=1}^{Nc} \{A_j^{(c)} J_0(\Lambda|\mathbf{r} - \mathbf{r}_j^{(c)}|) + B_j^{(c)} I_0(\Lambda|\mathbf{r} - \mathbf{r}_j^{(c)}|)\}, \tag{9}$$

where position vectors $\mathbf{r}_j^{(s)}$ and $\mathbf{r}_j^{(c)}$, respectively, indicate one of Ns source points on Γ_s and one of Nc source points on Γ_c ($N = Ns + Nc$).

In general, the assumed solution equation (9) should satisfy the boundary conditions (equations (4–7)) as well as the governing differential equation in order to become an eigensolution. Note that the assumed solution naturally satisfies the governing equation because it is made by a linear superposition of NDIFs satisfying the governing equation. However, only three boundary conditions (equations (4, 6, 7)) are considered and equation (5) is discarded in the paper. This approach will reduce numerical calculation effort because equation (5) is complex, compared with the other three boundary conditions.

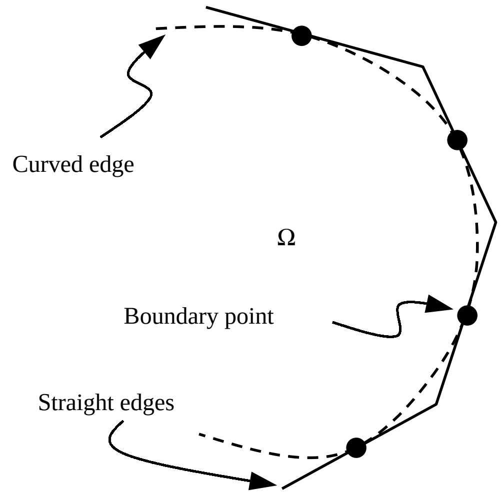

Figure 2. A curved edge approximated by many small straight edges, whose normal directions are equivalent to those of boundary points.

On the other hand, two boundary conditions (equations (4, 5)) should be considered to describe boundary conditions for simply supported *curved* edges. However, only one boundary condition (equation (4)) is employed for simply supported *straight* edges because equation (5) is automatically satisfied once equation (4) is satisfied. If delivering the fact that a curved edge can be approximated as many small straight edges as shown in Figure 2, it may be said that the discarding of equation (5) has a reasonable meaning even in the case of the paper dealing with curved edges as well as straight edges.

The selected boundary conditions (equations (4, 6, 7)) are applied to the assumed solution at boundary points (or source points) distributed along the boundaries Γ_s and Γ_c, using a kind of collocation technique (see Figure 1). Substituting Ns boundary points on Γ_s into equation (4) yields

$$W(\mathbf{r}_i^{(s)}) = \sum_{j=1}^{Ns} \{A_j^{(s)} J_0(\Lambda|\mathbf{r}_i^{(s)} - \mathbf{r}_j^{(s)}|) + B_j^{(s)} I_0(\Lambda|\mathbf{r}_i^{(s)} - \mathbf{r}_j^{(s)}|)\}$$
$$+ \sum_{j=1}^{Nc} \{A_j^{(c)} J_0(\Lambda|\mathbf{r}_i^{(s)} - \mathbf{r}_j^{(c)}|) + B_j^{(c)} I_0(\Lambda|\mathbf{r}_i^{(s)} - \mathbf{r}_j^{(c)}|)\} = 0, \quad i = 1, 2, \ldots, Ns \qquad (4^*)$$

and substituting Nc boundary points on Γ_c into equations (6, 7) yields

$$W(\mathbf{r}_i^{(c)}) = \sum_{j=1}^{Ns} \{A_j^{(s)} J_0(\Lambda|\mathbf{r}_i^{(c)} - \mathbf{r}_j^{(s)}|) + B_j^{(s)} I_0(\Lambda|\mathbf{r}_i^{(c)} - \mathbf{r}_j^{(s)}|)\}$$
$$+ \sum_{j=1}^{Nc} \{A_j^{(c)} J_0(\Lambda|\mathbf{r}_i^{(c)} - \mathbf{r}_j^{(c)}|) + B_j^{(c)} I_0(\Lambda|\mathbf{r}_i^{(c)} - \mathbf{r}_j^{(c)}|)\} = 0, \quad i = 1, 2, \ldots, Nc \qquad (6^*)$$

$$\frac{\partial W(\mathbf{r}_i^{(c)})}{\partial n_i} = \sum_{j=1}^{Ns} \left\{A_j^{(s)} \frac{\partial}{\partial n_i} J_0(\Lambda|\mathbf{r}_i^{(c)} - \mathbf{r}_j^{(s)}|) + B_j^{(s)} \frac{\partial}{\partial n_i} I_0(\Lambda|\mathbf{r}_i^{(c)} - \mathbf{r}_j^{(s)}|)\right\}$$
$$+ \sum_{j=1}^{Nc} \left\{A_j^{(c)} \frac{\partial}{\partial n_i} J_0(\Lambda|\mathbf{r}_i^{(c)} - \mathbf{r}_j^{(c)}|) + B_j^{(c)} \frac{\partial}{\partial n_i} I_0(\Lambda|\mathbf{r}_i^{(c)} - \mathbf{r}_j^{(c)}|)\right\} = 0, \quad i = 1, 2, \ldots, Nc. \qquad (7^*)$$

For simplicity, equations (4*, 6*, 7*) are, respectively, rewritten as three matrix equations:

$$\mathbf{SMJ}^{(ss)}\,\mathbf{A}^{(s)} + \mathbf{SMI}^{(ss)}\,\mathbf{B}^{(s)} + \mathbf{SMJ}^{(sc)}\,\mathbf{A}^{(c)} + \mathbf{SMI}^{(sc)}\,\mathbf{B}^{(c)} = \mathbf{0}, \tag{10}$$

$$\mathbf{SMJ}^{(cs)}\,\mathbf{A}^{(s)} + \mathbf{SMI}^{(cs)}\,\mathbf{B}^{(s)} + \mathbf{SMJ}^{(cc)}\,\mathbf{A}^{(c)} + \mathbf{SMI}^{(cc)}\,\mathbf{B}^{(c)} = \mathbf{0}, \tag{11}$$

$$\mathbf{VMJ}^{(cs)}\,\mathbf{A}^{(s)} + \mathbf{VMI}^{(cs)}\,\mathbf{B}^{(s)} + \mathbf{VMJ}^{(cc)}\,\mathbf{A}^{(c)} + \mathbf{VMI}^{(cc)}\,\mathbf{B}^{(c)} = \mathbf{0}, \tag{12}$$

where $\mathbf{SMJ}^{(ab)}$, $\mathbf{SMI}^{(ab)}$, $\mathbf{VMJ}^{(ab)}$ and $\mathbf{VMI}^{(ab)}$ ($a, b = s$ or c) are, respectively, given by

$$SMJ_{ij}^{(ab)} = J_0(\Lambda|\mathbf{r}_i^{(a)} - \mathbf{r}_j^{(b)}|), \qquad SMI_{ij}^{(ab)} = I_0(\Lambda|\mathbf{r}_i^{(a)} - \mathbf{r}_j^{(b)}|), \tag{13, 14}$$

$$VMJ_{ij}^{(ab)} = \frac{\partial}{\partial n_i} J_0(\Lambda|\mathbf{r}_i^{(a)} - \mathbf{r}_j^{(b)}|), \qquad VMI_{ij}^{(ab)} = \frac{\partial}{\partial n_i} I_0(\Lambda|\mathbf{r}_i^{(a)} - \mathbf{r}_j^{(b)}|). \tag{15, 16}$$

4. ADDITIONAL CONDITION FOR THE COMPLETE SYSTEM MATRIX

It should be pointed out that matrix equations (10–12) are incomplete because the number of unknown vectors $\mathbf{A}^{(s)}$, $\mathbf{A}^{(c)}$, $\mathbf{B}^{(s)}$ and $\mathbf{B}^{(c)}$ is 4 but the number of given equations is 3. This incompleteness results from the fact that one of the four boundary conditions is not considered and an additional equation is required. Thus, careful consideration is taken into equation (10), which has been made from the geometric boundary condition defined on simply supported edges. Referring to a previous research by the author [1], $\mathbf{SMI}^{(ss)}\,\mathbf{B}^{(s)}$ and $\mathbf{SMI}^{(sc)}\,\mathbf{B}^{(c)}$ in equation (10) may be removed because a general solution of fixed membranes or simply supported plates does not need them associated with the Bessel functions of order zero of second kind. On the basis of this fact, $\mathbf{SMI}^{(ss)}\,\mathbf{B}^{(s)}$ and $\mathbf{SMI}^{(sc)}\,\mathbf{B}^{(c)}$ are removed in the paper by using the following matrix equation:

$$\mathbf{SMI}^{(ss)}\,\mathbf{B}^{(s)} + \mathbf{SMI}^{(sc)}\,\mathbf{B}^{(c)} = \mathbf{0}, \tag{17}$$

which is chosen as an additional condition for completing the current incomplete boundary condition. In order to merge equation (17) into equations (10–12), equation (17) is changed in the form

$$\mathbf{B}^{(s)} = \mathbf{SMI}^{(ss)-1}\mathbf{SMI}^{(sc)}\,\mathbf{B}^{(c)}, \tag{18}$$

which is substituted into equations (10–12). Then,

$$\mathbf{SMJ}^{(ss)}\,\mathbf{A}^{(s)} + \mathbf{SMJ}^{(sc)}\,\mathbf{A}^{(c)} = \mathbf{0}, \tag{10*}$$

$$\mathbf{SMJ}^{(cs)}\,\mathbf{A}^{(s)} + \mathbf{SMJ}^{(cc)}\,\mathbf{A}^{(c)} + (\mathbf{SMI}^{(cc)} - \mathbf{SMI}^{(cs)}\mathbf{SMI}^{(ss)-1}\mathbf{SMI}^{(sc)})\mathbf{B}^{(c)} = \mathbf{0}, \tag{11*}$$

$$\mathbf{VMJ}^{(cs)}\,\mathbf{A}^{(s)} + \mathbf{VMJ}^{(cc)}\,\mathbf{A}^{(c)} + (\mathbf{VMI}^{(cc)} - \mathbf{VMI}^{(cs)}\mathbf{SMI}^{(ss)-1}\mathbf{SMI}^{(sc)})\mathbf{B}^{(c)} = \mathbf{0}. \tag{12*}$$

Three matrix equations (10*–12*) can be assembled into one matrix equation:

$$\mathbf{SM}(\Lambda)\mathbf{C} = \mathbf{0}, \tag{19}$$

where the square matrix $\mathbf{SM}(\Lambda)$ of order $Ns + 2Nc$ is the system matrix of a plate with the mixed boundary condition, and is a function of the frequency parameter Λ. Here, the system matrix $\mathbf{SM}(\Lambda)$ and the unknown vector $\mathbf{C}$ are given by

$$\mathbf{SM}(\Lambda) = \begin{bmatrix} \mathbf{SMJ}^{(ss)} & \mathbf{SMJ}^{(sc)} & \mathbf{0} \\ \mathbf{SMJ}^{(cs)} & \mathbf{SMJ}^{(cc)} & \mathbf{EMI}^{(cc)} \\ \mathbf{VMJ}^{(cs)} & \mathbf{VMJ}^{(cc)} & \mathbf{FMI}^{(cc)} \end{bmatrix}, \qquad \mathbf{C} = \begin{Bmatrix} \mathbf{A}^{(s)} \\ \mathbf{A}^{(c)} \\ \mathbf{B}^{(c)} \end{Bmatrix}, \tag{20, 21}$$

where

$$\mathbf{EMI}^{(cc)} = \mathbf{SMI}^{(cc)} - \mathbf{SMI}^{(cs)}\mathbf{SMI}^{(ss)-1}\mathbf{SMI}^{(sc)}, \tag{22}$$

$$\mathbf{FMI}^{(cc)} = \mathbf{VMI}^{(cc)} - \mathbf{VMI}^{(cs)}\mathbf{SMI}^{(ss)-1}\mathbf{SMI}^{(sc)}. \tag{23}$$

In order to obtain the singular values of the system matrix $\mathbf{SM}(\Lambda)$, the determinant det($\mathbf{SM}$) of the system matrix is swept in the frequency range of interest. Singular values corresponding to eigenvalues $\Lambda_1, \Lambda_2, \ldots, \Lambda_k, \ldots$ can be found from determinant curves. Furthermore, the kth eigenvector can be computed with the kth eigenvalue Λ_k obtained from a determinant curve. On substituting Λ_k into the system equation (19), $\mathbf{C}_{k\text{th}} = \{\mathbf{A}^{(s)}_{k\text{th}} \ \ \mathbf{A}^{(c)}_{k\text{th}} \ \ \mathbf{B}^{(c)}_{k\text{th}}\}^{\mathrm{T}}$ corresponding to a part of the kth eigenvector can be extracted. In addition, unknown vector $\mathbf{B}^{(s)}_{k\text{th}}$ can also be calculated by substituting $\mathbf{B}^{(c)}_{k\text{th}}$ given by $\mathbf{C}_{k\text{th}}$ into equation (18), i.e., $\mathbf{B}^{(s)}_{k\text{th}} = \mathbf{SMI}^{(ss)-1}\mathbf{SMI}^{(sc)}\ \mathbf{B}^{(s)}_{k\text{th}}$. Finally, the shape of the kth mode can be plotted by substituting $\mathbf{A}^{(s)}_{k\text{th}}$, $\mathbf{A}^{(c)}_{k\text{th}}$, $\mathbf{B}^{(s)}_{k\text{th}}$ and $\mathbf{B}^{(c)}_{k\text{th}}$ into equation (9).

5. TREATMENT OF SPURIOUS SINGULAR VALUES

In this section, a discussion on spurious singular values is given using a rectangular plate with the mixed boundary condition as shown in Figure 3. Logarithm values of det[$\mathbf{SM}(\Lambda)$] for the rectangular plate are swept in the range of $\Lambda = 4{\cdot}5$–12 as shown in Figure 4 where troughs SV_ks represent singular values of the system matrix $\mathbf{SM}$ and the singular values obtained here are summarized in Table 1. It may be confirmed in Table 1 that when the singular values are compared to the FEM results or Leissa's results, only a part (SV_2, SV_4, SV_7, SV_9, SV_{10} and SV_{13}) of the singular values corresponds to the eigenvalues of the plate with the mixed boundary condition. Thus, other singular values may be considered as spurious singular values, which correspond to the eigenvalues of the similarly shaped simply supported plate (see Table 1).

The reason for the appearance of these spurious singular values can be demonstrated by investigating the system matrix given in equation (20). The determinant of the system matrix

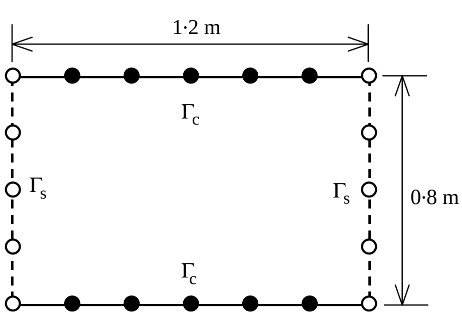

Figure 3. Rectangular plate with the SSCC boundary condition: its boundary is discretized with 20 boundary points.

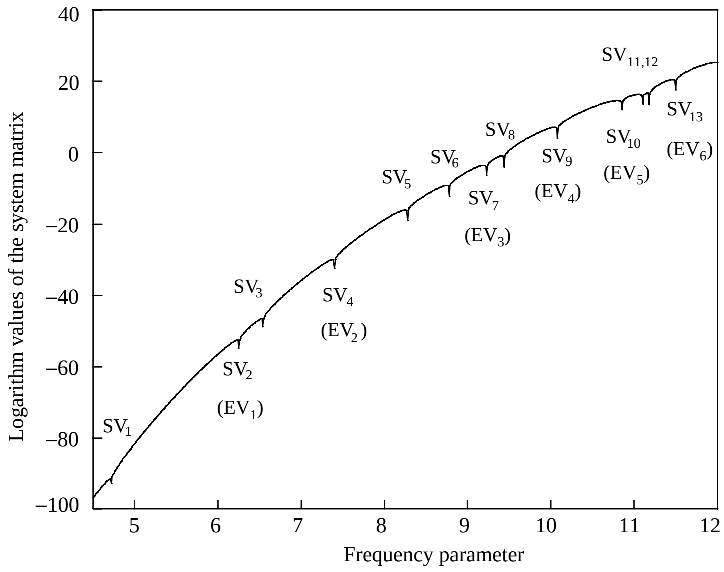

Figure 4. Logarithm curve for det[**SM**] of the rectangular plate with the SSCC boundary condition.

TABLE 1

Comparison between singular values and eigenvalues of the rectangular plate with the SSCC boundary condition

		Simply supported B.C.		Mixed B.C.		
Singular values	det(**SM**)	det(**SMJ**)	Exact	det(**SM**)/det(**SMJ**)	FEM	Leissa
SV_1	4·72	4·72	4·72			
SV_2	6·25			6·25 (EV_1)	6·25	6·26
SV_3	6·54	6·54	6·55			
SV_4	7·40			7·40 (EV_2)	7·40	7·41
SV_5	8·28	8·28	8·28			
SV_6	8·78	8·78	8·78			
SV_7	9·23			9·23 (EV_3)	9·24	9·25
SV_8	9·44	9·44	9·44			
SV_9	10·08			10·1 (EV_4)	10·1	10·1
SV_{10}	10·86			10·9 (EV_5)	10·9	10·9
SV_{11}	11·11	11·11	11·11			
SV_{12}	11·18	11·18	11·18			
SV_{13}	11·50			11·5 (EV_6)	11·5	11·5

may be interpreted in an alternative way:

$$\det(\mathbf{SM}) \Leftrightarrow \det(\mathbf{FMI}^{(cc)})\det(\mathbf{SMJ}) + \det(\mathbf{EMI}^{(cc)})\det(\mathbf{GMJ}), \tag{24}$$

where

$$\mathbf{SMJ} = \begin{bmatrix} \mathbf{SMJ}^{(ss)} & \mathbf{SMJ}^{(sc)} \\ \mathbf{SMJ}^{(cs)} & \mathbf{SMJ}^{(cc)} \end{bmatrix}, \qquad \mathbf{GMJ} = \begin{bmatrix} \mathbf{SMJ}^{(ss)} & \mathbf{SMJ}^{(sc)} \\ \mathbf{VMJ}^{(cs)} & \mathbf{VMJ}^{(cc)} \end{bmatrix}. \tag{25, 26}$$

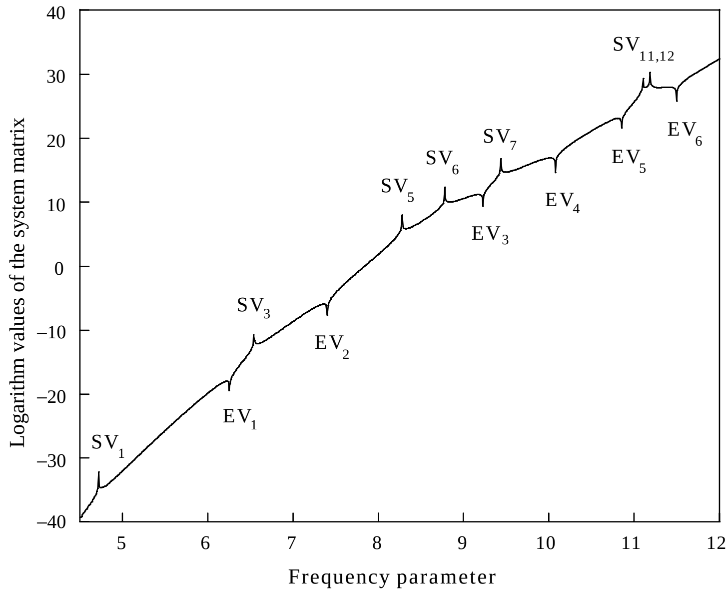

Figure 5. Logarithm curve for det[**SM**]/det[**SMJ**] of the rectangular plate with the SSCC boundary condition.

It should be noted that **SMJ** represents the system matrix of the similarly shaped simply supported plate or fixed membrane [1], and that **GMJ**(1, 1)and **GMJ**(1, 2) of four sub-matrices involved in **GMJ** are equivalent to **SMJ**(1, 1) and **SMJ**(1, 2). Furthermore, **GMJ**(2, 1)and **GMJ**(2, 2) are equivalent to **VMJ**(2, 1) and **VMJ**(2, 2) involved in $\mathbf{VMJ} = \partial(\mathbf{SMJ})/\partial n$:

$$\mathbf{VMJ} = \begin{bmatrix} \mathbf{VMJ}^{(ss)} & \mathbf{VMJ}^{(sc)} \\ \mathbf{VMJ}^{(cs)} & \mathbf{VMJ}^{(cc)} \end{bmatrix}. \tag{27}$$

On referring to previous research [3], some of the singular values of **VMJ** are identical to the singular values of **SMJ**. As a result, **GMJ** whose elements correspond to elements of both **SMJ** and **VMJ** also has the same singular values as **SMJ**. From this fact, the determinant of **GMJ** may be written as

$$\det(\mathbf{GMJ}) = \det(\mathbf{SMJ}) f(\Lambda), \tag{28}$$

where $f(\Lambda)$ denotes a residual function. Note that singular values of **GMJ** are obtained from two equations: $\det(\mathbf{SMJ}) = 0$ and $f(\Lambda) = 0$. Finally, substituting equation (28) into equation (24) yields

$$\det(\mathbf{SM}) = \det(\mathbf{SMJ})[\det(\mathbf{FMI}^{(cc)}) + \det(\mathbf{EMI}^{(cc)}) f(\Lambda)]. \tag{29}$$

From equation (29), it may be concluded that the system matrix **SM** automatically becomes singular when **SMJ** is singular, i.e., if $\det(\mathbf{SMJ}) = 0$, $\det(\mathbf{SM}) = 0$. Thus, the singular values of **SMJ** appear in the determinant curve of the system matrix **SM** as shown in Figure 4. On the other hand, the same method as in the previous research [5] is applied to discriminate between correct singular values and spurious ones. The logarithm curve for det[**SM**]/det[**SMJ**] is plotted in Figure 5 where troughs and crests represent the eigenvalues of the plate with the mixed boundary condition and those of the similar shaped simply supported plate respectively.

6. VERIFICATION EXAMPLES

6.1. RECTANGULAR PLATE WITH THE MIXED BOUNDARY CONDITION (C-S-S-C)

Figure 6 shows a rectangular plate with the CSSC boundary condition that the left and right edges are subject to the clamped boundary condition and the simply supported one, respectively, and the upper and lower edges are subject to the simply supported boundary condition and the clamped one. Note that the normal direction n_{ave} at the corner between the two clamped edges is approximated by the vector sum of the normal directions of the two edges (see Figure 6).

Logarithm curves for both det[**SM**]/det[**SMJ**] and det[**SM**] are shown in Figure 7, where it may be seen that spurious singular values are successfully removed. Furthermore, it may be said from Table 2 that, although only 18 boundary points are used, the eigenvalues

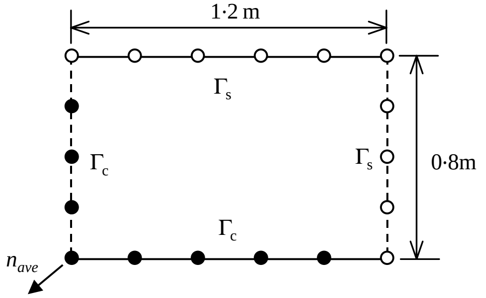

Figure 6. Rectangular plate with the CSSC boundary condition: its boundary is discretized with 18 boundary points.

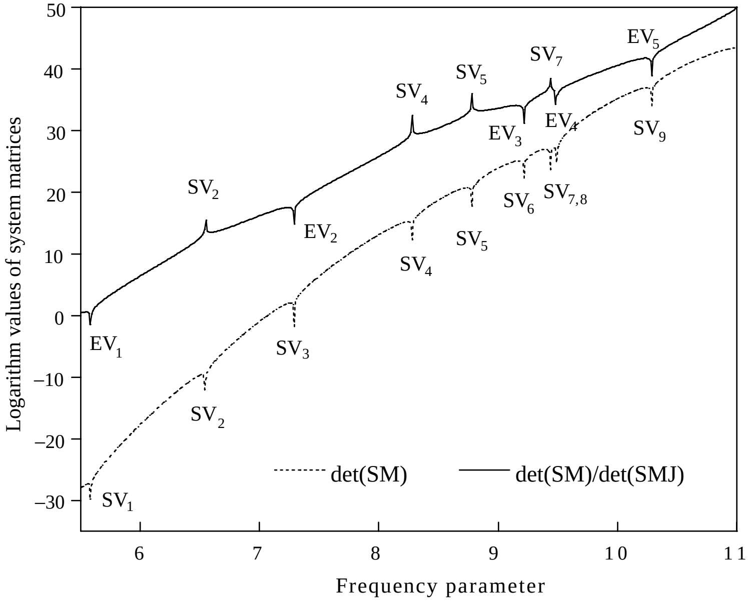

Figure 7. Logarithm curves for det[**SM**] and det[**SM**]/det[**SMJ**] of the rectangular plate with the CSSC boundary condition.

TABLE 2

Eigenvalues of the rectangular plate with the CSSC boundary condition, obtained by the proposed method, Leissa's method, and FEM (ANSYS)

Singular values	det(**SM**)	Simply supported B.C. det(**SMJ**)	Simply supported B.C. Exact	Mixed B.C. det(**SM**)/det(**SMJ**)	FEM	Leissa
SV_1	5·58			5·58 (EV_1)	5·58	5·58
SV_2	6·54	6·54	6·55			
SV_3	7·29			7·29 (EV_2)	7·29	7·29
SV_4	8·28	8·28	8·28			
SV_5	8·78	8·78	8·78			
SV_6	9·22			9·22 (EV_3)	9·21	9·22
SV_7	9·44	9·44	9·44			
SV_8	9·49			9·49 (EV_4)	9·47	9·48
SV_9	10·3			10·3 (EV_5)	10·3	10·3

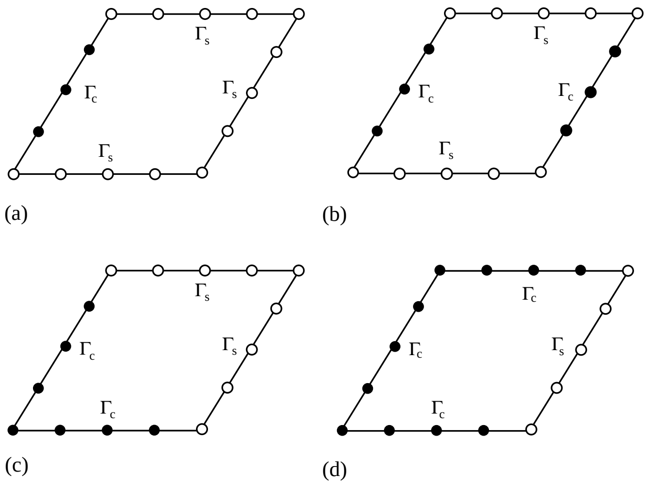

Figure 8. Rhombic plates with various combinations of boundary conditions: (a) CSSS, (b) CCSS, (c) CSSC, (d) CSCC.

TABLE 3

Eigenvalues and errors (%) of rhombic plates with various boundary conditions, obtained by the proposed method, Nair's method, and FEM (ANSYS)

Eigenvalues	Proposed	FEM	Nair	Proposed	FEM	Nair
	CSSS B.C.			CCSS B.C.		
EV_1	6·81 (– 0·44)	6·84	6·94 (1·46)	7·55 (– 0·53)	7·59	7·65 (0·79)
EV_2	9·56 (– 0·10)	9·57	9·66 (0·94)	9·96 (– 0·40)	10·0	10·1 (1·00)
EV_3	11·1 (– 0·89)	11·2	11·3 (0·89)	11·9 (– 0·83)	12·0	12·1 (0·83)
EV_4	11·9 (– 0·83)	12·0	12·1 (0·83)	12·5 (0·00)	12·5	12·6 (0·80)
	CSSC B.C.			CSCC B.C.		
EV_1	7·24 (– 0·69)	7·29	7·37 (1·10)	7·93 (– 0·25)	7·95	8·00 (0·63)
EV_2	10·2 (0·00)	10·2	10·2 (0·00)	10·7 (0·00)	10·7	10·7 (0·00)
EV_3	11·5 (– 0·86)	11·6	11·8 (1·72)	12·2 (– 0·81)	12·3	12·4 (0·81)
EV_4	12·5 (0·00)	12·5	12·6 (0·80)	13·0 (– 0·76)	13·1	13·2 (0·76)

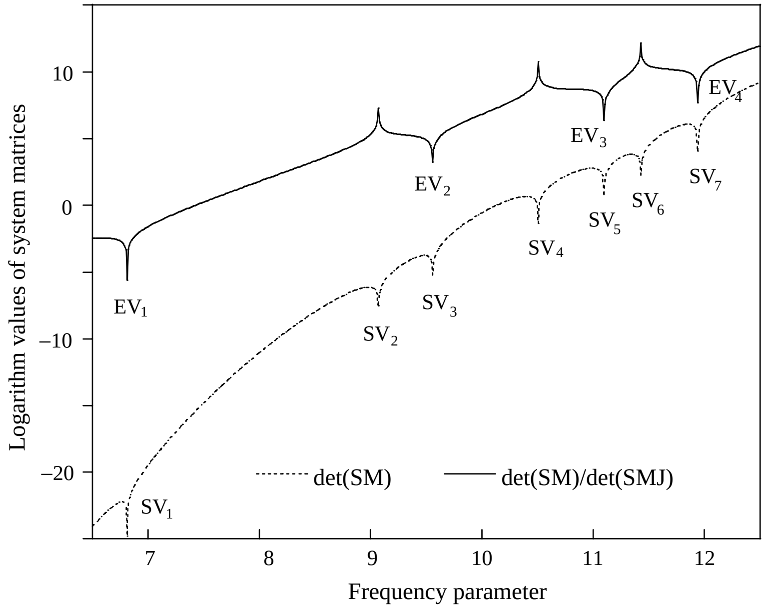

Figure 9. Logarithm curves for det[**SM**] and det[**SM**]/det[**SMJ**] of the rhombic plate with the CSSS boundary condition.

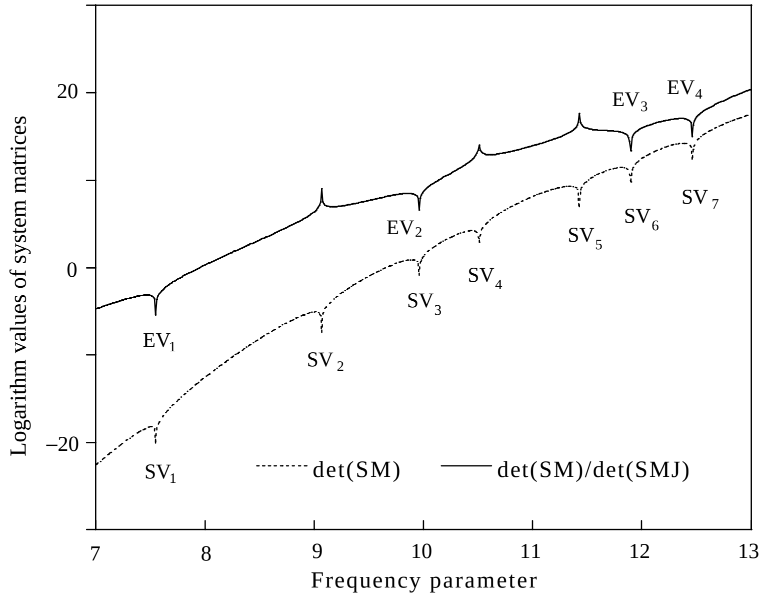

Figure 10. Logarithm curves for det[**SM**] and det[**SM**]/det[**SMJ**] of the rhombic plate with the CCSS boundary condition.

obtained by the proposed method agree well with those calculated by the FEM results and Leissa's results [19].

6.2. RHOMBIC PLATES WITH MIXED BOUNDARY CONDITIONS

Figure 8 shows rhombic plates with various combinations of boundary conditions. Logarithm curves for the rhombic plates are shown in Figures 9–12 and eigenvalues for

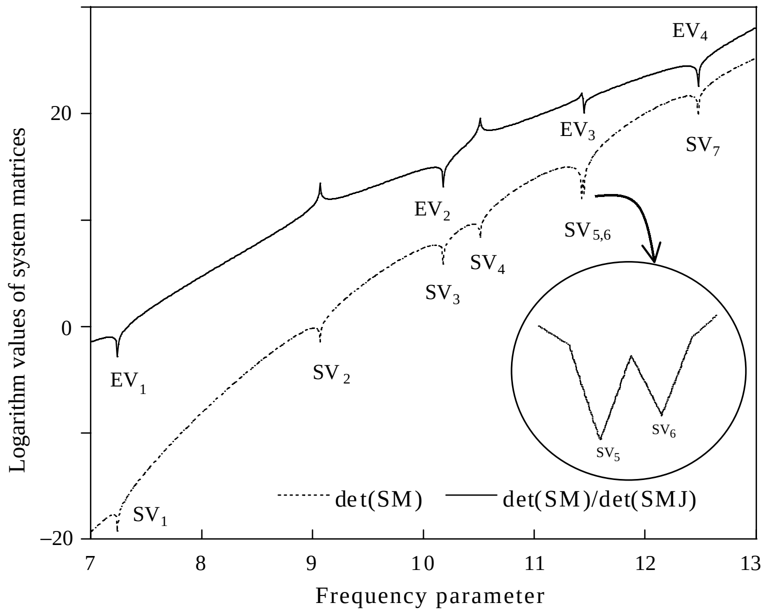

Figure 11. Logarithm curves for det[**SM**] and det[**SM**]/det[**SMJ**] of the rhombic plate with the CSSC boundary condition.

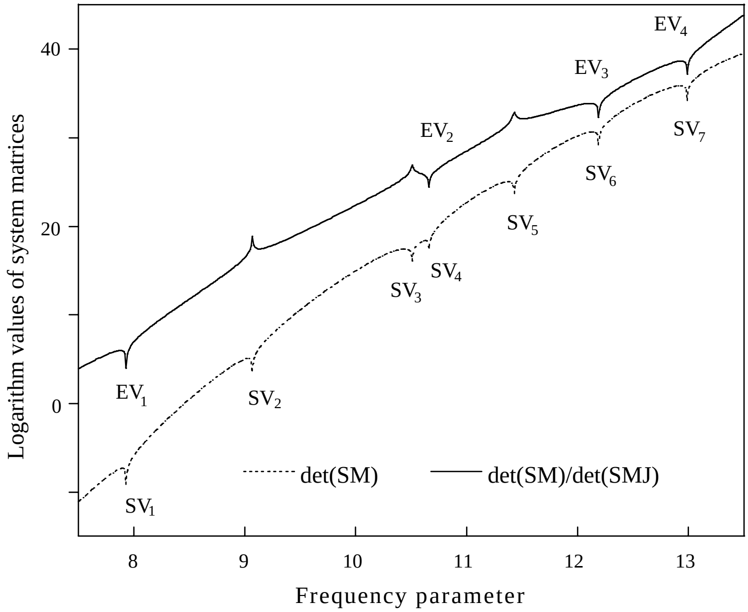

Figure 12. Logarithm curves for det[**SM**] and det[**SM**]/det[**SMJ**] of the rhombic plate with the CSCC boundary condition.

each plate are summarized in Table 3. As can be seen from the figures, troughs corresponding to spurious singular values are successfully eliminated by means of the proposed approach, for all possible combinations of boundary conditions. Furthermore, it

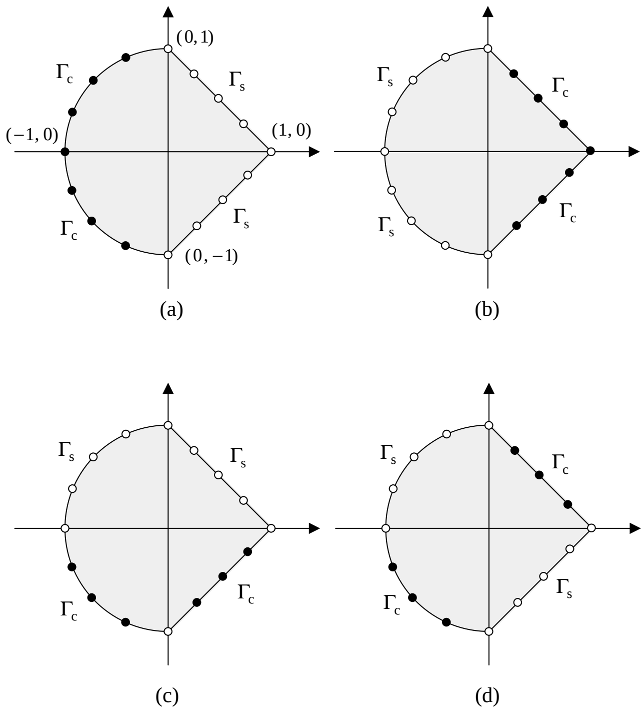

Figure 13. Arbitrarily shaped plates with various combinations of boundary conditions: (a) CSCS, (b) SCSC, (c) CSSC, (d) CCSS.

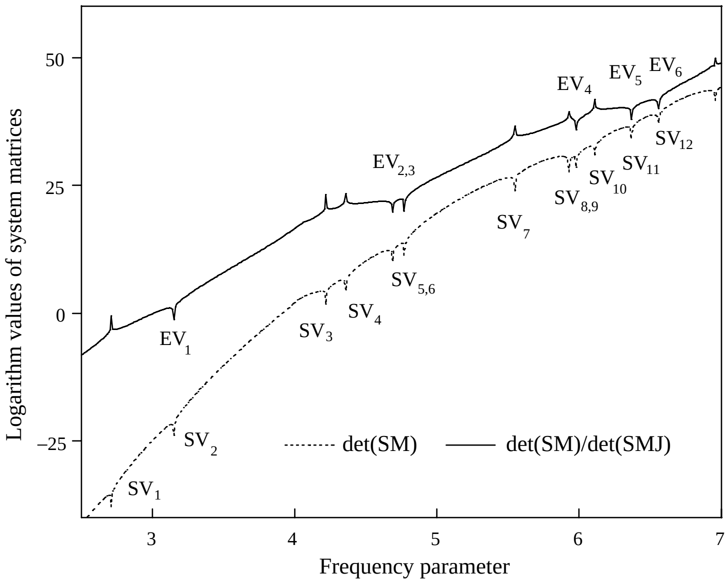

Figure 14. Logarithm curves for det[**SM**] and det[**SM**]/det[**SMJ**] of the rhombic plate with the CSCS boundary condition.

may be said that the eigenvalues obtained by the proposed method have an extremely small amount of error and are more accurate than Nair's results, compared with the FEM results using 441 nodes, which will give solutions nearly close to exact values.

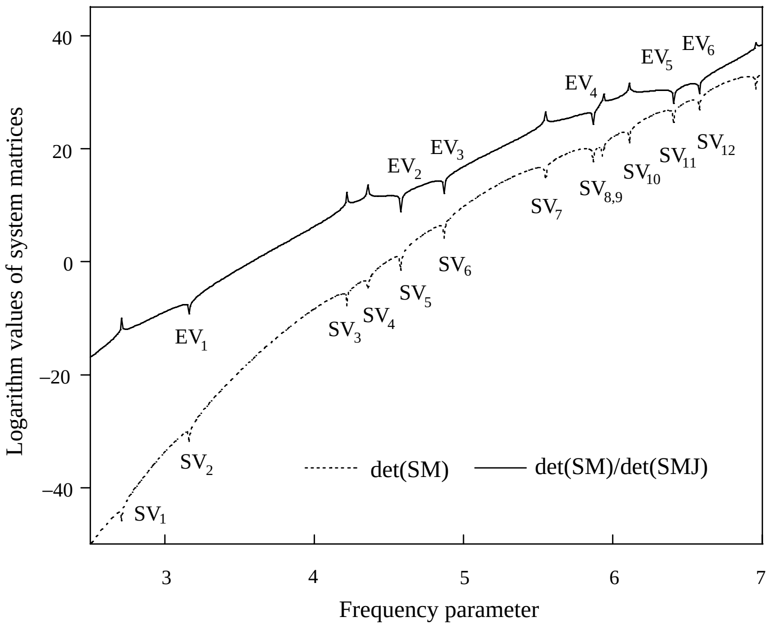

Figure 15. Logarithm curves for det[**SM**] and det[**SM**]/det[**SMJ**] of the rhombic plate with the SCSC boundary condition.

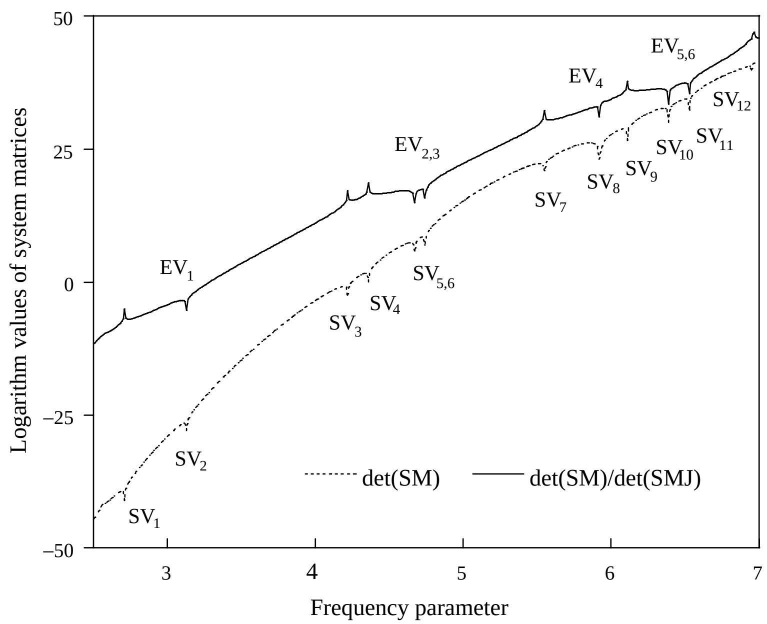

Figure 16. Logarithm curves for det[**SM**] and det[**SM**]/det[**SMJ**] of the rhombic plate with the CSSC boundary condition.

6.3. ARBITRARILY SHAPED PLATE

Figure 13 shows various combinations of mixed boundary conditions applied to an arbitrarily shaped plate defined in the paper. Associated determinant curves are given in

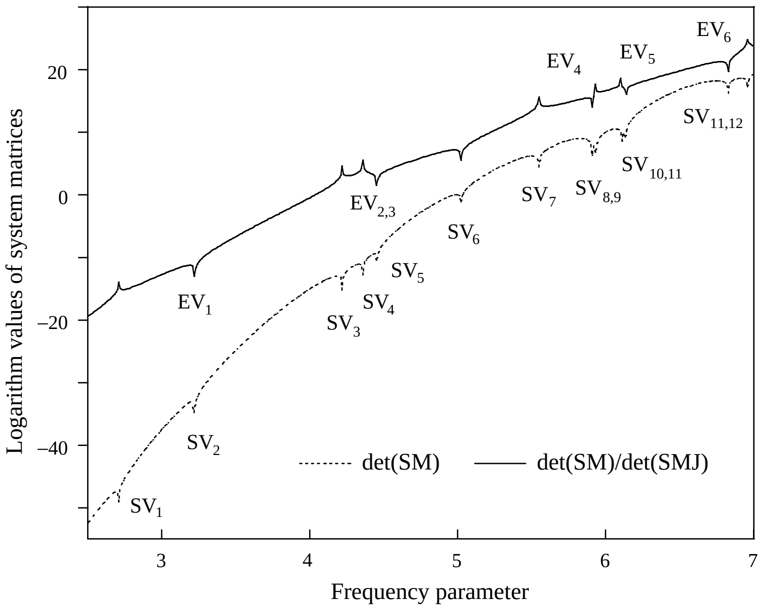

Figure 17. Logarithm curves for det[**SM**] and det[**SM**]/det[**SMJ**] of the rhombic plate with the CCSS boundary condition.

TABLE 4

Eigenvalues and errors (%) of the arbitrarily shaped plate with various boundary conditions, obtained by the proposed method and FEM (ANSYS)

	CSCS B.C.		SCSC B.C.		CSSC B.C.		CCSS B.C.	
Eigenvalues	Proposed	FEM	Proposed	FEM	Proposed	FEM	Proposed	FEM
EV_1	3·15 (− 0·32)	3·16	3·16 (1·61)	3·11	3·13 (0·00)	3·13	3·22 (− 0·92)	3·25
EV_2	4·69 (− 0·85)	4·73	4·58 (0·44)	4·56	4·67 (0·65)	4·64	4·45 (− 0·22)	4·46
EV_3	4·77 (0·00)	4·77	4·87 (0·83)	4·83	4·74 (− 1·04)	4·79	5·02 (− 0·99)	5·07
EV_4	5·98 (− 0·99)	6·04	5·87 (− 0·51)	5·90	5·92 (− 0·84)	5·97	5·91 (− 1·34)	5·99
EV_5	6·37 (0·00)	6·37	6·41 (0·47)	6·38	6·39 (0·31)	6·37	6·13 (0·00)	6·13
EV_6	6·56 (− 0·30)	6·58	6·58 (0·46)	6·55	6·53 (− 0·31)	6·55	6·83 (− 0·29)	6·85

Figures 14–17 where singular values labelled by EV_1–EV_6 correspond to eigenvalues. The figures show that the proposed way of filtering out incorrect singular values is valid and effective. In addition, it may be said in Table 4 that the eigenvalues obtained agree well with the FEM result using 663 nodes and most of the errors are within 1%, compared with the corresponding FEM results.

7. CONCLUSIONS

The new method for free vibration analysis of arbitrarily shaped plates with mixed boundary conditions described in this paper is efficient and accurate. The method needs no numerical integral procedure on boundaries and it requires a small amount of numerical calculation due to the discarding of the natural boundary condition given on simply supported edges. Although employing incomplete boundary conditions, the method gives valid and accurate results due to the additional boundary condition devised in the study. On the other hand, the proposed method may be extended to the free vibration analysis of membranes and plates with non-homogeneity in thickness and material properties, and related work is being carried out for another paper.

ACKNOWLEDGMENTS

This research was financially supported by Hansung University in the year 2001.

REFERENCES

1. S. W. KANG, J. M. LEE and Y. J. KANG 1999 *Journal of Sound and Vibration* **221**, 117–132. Vibration analysis of arbitrarily shaped membranes using non-dimensional dynamic influence function.
2. S. W. KANG and J. M. LEE 2000 *Journal of Sound and Vibration* **235**, 170–171. Authors' reply (comments on "Vibration analysis of arbitrary shaped membranes using non-dimensional dynamic influence function").
3. S. W. KANG and J. M. LEE 2000 *Journal of the Acoustical Society of America* **107**, 1153–1160. Eigenmode analysis of arbitrarily shaped two-dimensional cavities by the method of point-matching.
4. S. W. KANG and J. M. LEE 2000 *Journal of Sound and Vibration* **234**, 455–470. Application of free vibration analysis of membranes using the non-dimensional dynamic influence function.
5. S. W. KANG and J. M. LEE 2001 *Journal of Sound and Vibration* **242**, 9–26. Free vibration analysis of arbitrarily shaped plates with clamped edges using wave-type functions.
6. H. D. CONWAY 1961 *American Society of Mechanical Engineers Journal of Applied Mechanics* **28**, 288–291. The bending, buckling, and flexural vibration of simply supported polygonal plates by point-matching.
7. B. SINGH and S. CHAKRAVERTY 1992 *Journal of Sound and Vibration* **152**, 149–155. Transverse vibration of simply supported elliptical and circular plates using boundary characteristic orthogonal polynomials in two variables.
8. H. D. CONWAY and K. A. KARNHAM 1965 *International Journal of Mechanical Sciences* **7**, 811–816. The free flexural vibration of triangular, rhombic and parallelogram plates and some analogies.
9. J. MAZUMDAR 1973 *Journal of Sound and Vibration* **27**, 47–57. Transverse vibration of membranes of arbitrary shape by the method of constant-deflection contours.
10. K. NAGAYA 1978 *American Society of Mechanical Engineers Journal of Applied Mechanics* **45**, 153–158. Vibrations and dynamic response of membranes with arbitrary shape.
11. S. DURVASULA 1969 *Journal of Aircraft* **6**, 66–68. Free vibration of simply supported parallelogrammic plates.
12. I. CHOPRA and S. DURVASULA 1972 *Journal of Sound and Vibration* **19**, 379–392. Vibration of simply supported trapezoidal plates, I. Symmetric trapezoids.
13. I. CHOPRA and S. DURVASULA 1972 *Journal of Sound and Vibration* **20**, 125–134. Vibration of simply supported trapezoidal plates, II. Unsymmetric trapezoids.
14. S. DURVASULA 1968 *Journal of the Acoustical Society of America* **44**, 1636–1646. Natural frequencies and modes of skew membranes.
15. S. DURVASULA 1969 *American Institute of Aeronautics and Astronautics Journal* **7**, 1164–1167. Natural frequencies and modes of clamped skew plates.
16. M. HASEGWA 1957 *Journal of Aeronautical Sciences* **24**, 145–146. Vibration of clamped parallelogrammic isotropic flat plates.
17. M. HAMADA 1959 *Bullitin of Japan Society of Mechanical Engineers* **2**, 520–526. Compressive or shear buckling load and fundamental frequency of a rhombioidal plate with all edges clamped.
18. P. S. NAIR and S. DURVASULA 1973 *Journal of Sound and Vibration* **26**, 1–19. Vibration of skew plates.

19. A. W. LEISSA 1973 *Journal of Sound and Vibration* **31**, 257–293. The free vibration of rectangular plates.
20. S. M. DICKINSON 1978 *Journal of Sound and Vibration* **61**, 1–8. The buckling and frequency of flexural vibration of rectangular, isotropic and orthotropic plates using Rayleigh's method.
21. R. SCHINZINGER and P. A. A. LAURA 1991 *Conformal Mapping: Methods and Applications*. New York: Elsevier Science Publishers.
22. P. A. A. LAURA 1972 Institute of Electrical and Electronic Engineers Transactions on Microwave Theory and Techniques **MTT-20**, 292. The solution of Helmholtz equation in elliptical coordinates.
23. P. A. SHAHADY, R. PASSARELLI and P. A. A. LAURA 1967 *Journal of the Acoustical Society of America* **42**, 806–809. Applications of complex-variable theory to the determination of the fundamental frequency of vibrating plates.
24. P. A. A. LAURA, E. ROMANELLI and M. J. MAURIZI 1972 *Journal of Sound and Vibration* **20**, 7–38. The analysis of waveguides of doubly-connected cross-section by the method of conformal mapping.
25. L. MEIROVITCH 1967 *Analytical Methods in Vibrations*, pp. 179–189. New York: Macmillan Publishing.